Design and fabrication of As2S3-based nonquarterwave multi-cavity Fabry-Perot filters with laser-adjustable central wavelength

Antoine Bourgade, Frederic Lemarquis, Antonin Moreau, Julien Lumeau

Design and fabrication of As2S3-based non-quarterwave multi-cavity Fabry-Perot filters with laser-adjustable central wavelength

ANTOINE BOURGADE, FREDERIC LEMARQUIS, ANTONIN MOREAU, THOMAS BEGOU AND JULIEN LUMEAU*

Aix Marseille Univ, CNRS, Centrale Marseille, Institut Fresnel, Marseille, France
**Corresponding author: julien.lumeau@fresnel.fr*

Received XX Month XXXX; revised XX Month, XXXX; accepted XX Month XXXX; posted XX Month XXXX (Doc. ID XXXXX); published XX Month XXXX

We present a thorough study of the use of As_2S_3 thin films for the fabrication of high performance multi-cavity bandpass filters. We show that such layers can be used inside a non-quarterwave multi-cavity Fabry-Perot structure to produce local changes of the central wavelength of the filter using photosensitive properties of this material. In particular, we study the impact of these index changes on the spectral performances of the filters and show how to adapt the design of the Fabry-Perot structures to produce a spectral shift without degrading the bandpass profile. Double and three-cavity Fabry-Perot filters are theoretically and experimentally studied. © 2022 Optical Society of America

OCIS codes: *(160.5335) Photosensitive materials; (310.6845) Thin film devices and applications*

http://dx.doi.org/10.1364/OL.99.099999

Thanks to the improvement of the deposition techniques and especially the associated optical monitoring systems, it is now more and more common to fabricate high performance filters with very stringent requirements and spectral performances close to that were designed. However, these spectral performances can be different within the aperture of the filter or in between filters due to uniformity problems associated with different distribution of deposited materials within the aperture of a substrate. As of today, the best deposition techniques allow securing a close to 0.1% change of the thickness over a 100 mm aperture [1], but most of the standard deposition techniques based on evaporation or sputtering are generally resulting in uniformities within the 1%-range such as it is not possible to fabricate large aperture filters with identically similar performances. Such uniformity problems are not such an issue when it comes to broadband spectral functions such as quarter-wave mirrors or broadband antireflection coatings but can become a major issue for local spectral functions such as narrow-bandpass filters for space or telecom applications.

Indeed, for achieving such spectral functions, quarterwave Fabry-Perot structures are generally used, and, as it was shown in ref. [2], that uniformity can highly affect the central wavelength of the bandpass proportionally to the change of thickness of all the layers. In addition, it was also shown that while a spectral shift can be due to thickness non-uniformity defect affecting all layers, a similar effect can be obtained by changing the thickness of a single layer. The cavity-layer is the most sensitive one for that, and it can be shown [2] that the relative variation of the central wavelength (λ) is proportional to the relative variation of the its optical thickness (nt). For this reason, the use cavity layers formed with materials which optical thickness can be changed after deposition is a promising approach to overcome these limitations. This concept was introduced some time ago [3], a basic proof-of-concept was published about 10 years ago [4] and complete demonstration has been recently published [5]. This approach relies on the fabrication of bandpass filters made with photosensitive cavity-layers in order to locally correct the central wavelength of the filter using photo-induced refractive index change. However, in refs. [4,5], only single cavity Fabry-Perot filters were studied. In this paper we first present why this method cannot be simply transferred to double cavity Fabry-Perot filters and how to overcome these limitations by adapting the filter design and the exposure wavelength to produce the desired spectral shift without any unexpected effect. We then show that it can be extended to a larger number of cavities. For each configuration, both theoretical analysis and experimental demonstration are provided.

The combination of several Fabry-Perot cavities is a classical structure that is commonly used for the production of bandpass filters with squared profiles and large rejection close to the bandpass. The number of cavities highly depends on the filters requirements but very often, it is comprised between 2 and 5. For optimum optical performances, each of the cavities needs to be accurately centered at the same wavelength, and this is generally

achieved by using turning point monitoring in order to benefit from error self-compensation associated with this method [6,-8]. However, this does not prevent from having a non-uniform distribution of the central wavelength over the filter aperture. To overcome this difficulty, we investigated how the use of photosensitive layers can be implemented in order to correct, after filter fabrication, the local central wavelength of multi-cavity Fabry-Perot filters. The first step consisted in the direct implementation of the results that are presented in ref. [5] and fabricating standard Fabry-Perot structures made of quarter-wave layers, cavity layers being made of photosensitive materials. The filter that we considered has the following structure:

M6/2C/M6*/L/M6/2C/M6*

where M6 and M6* represent mirrors made of 6 alternated high (H: ZnS) and low (L: YF_3) refractive index materials quarter-wave layers at 808 nm, with exact formula: M6 – HLHLHL and M6* - LHLHLH, and 2C is an As_2S_3 half-wave layer at 808 nm. Such a filter was fabricated on a Bühler SYRUSpro 710 deposition machine using an electron beam deposition associated with a Bühler OMS 5000 optical monitoring system and turning point monitoring at 808 nm. The filters were deposited at room temperature on fused silica substrates and the transmission was measured on a Perkin Elmer Lambda 1050 spectrophotometer. One can see that the filter is centered at 808 nm confirming that error compensation due to turning point monitoring strategy was efficient and that no significant vacuum/air shift occurred as the filter was monitored using turning point monitoring at the same wavelength. Then, the filters have been exposed to the radiation from a Thorlabs pigtailed LED at 470 nm similar to the source that was used in ref. [5]. The filters transmittance spectra have been measured after different increasing exposure dosages (D1 to D4) and plotted in Figure 1. Due to the nonlinearity of the refractive index change on dosage, the durations were adjusted to secure approximately ¼, ½, ¾ and 1× of the maximum refractive index change for the respective exposure dosage D1, D2, D3 and D4.

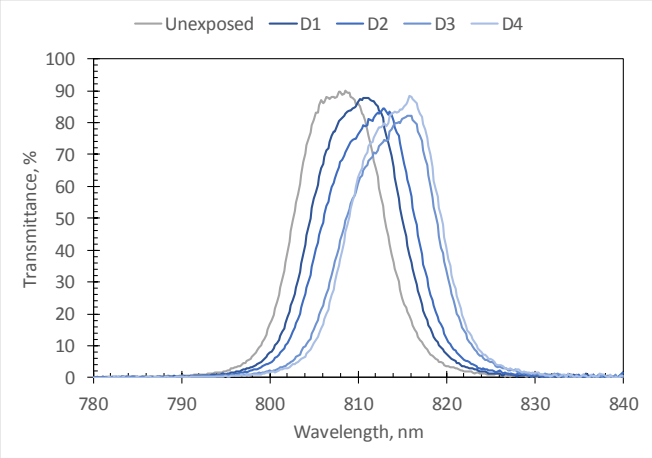

Figure 1. Experimental evolution of the transmittance of a two-cavity quarter-wave layers bandpass filters for increasing of dosage of exposure at 470 nm (from a dosage D1 to D4).

As expected, exposing the filter at 470 nm produces a shift of the bandpass central wavelength towards the longer wavelengths. The filter shifts by about 10 nm from 808 nm up to 818 nm. This represent 1.2% change of the central wavelength, which is enough to compensate a standard 1% non-uniformity defect. It is interesting to note that this wavelength variation is lower than the refractive index change which can reach 3.3% at 808 nm.

Initially, the filter shows a symmetrical profile with slightly rounded transmission at maximum. However, one can notice, during the exposure, an induced distortion of the bandpass as well as a decrease of the maximum transmission, which is typical of detuned cavities. This distortion can be easily explained by looking at the electric field distribution at 470 nm. Indeed, modeling the intensity distribution of electric field inside the filter shows that it is about 3 times lower inside the second cavity than that in the first one, because of interferences and also because of absorption in As_2S_3 at 470 nm. As a consequence, due to the kinetics of photosensitivity of the As_2S_3 layers [5], the first cavity tends to shift faster than the second one, resulting in a mismatch between the central wavelengths of the two cavities and therefore a distortion of the spectral profile in the bandpass region. To illustrate this effect, we modeled in Figure 2 the expected shift of the bandpass taking into account the intensity distribution in the cavities and the photosensitivity curve for similar dosage to that used for producing the curves in Figure 1.

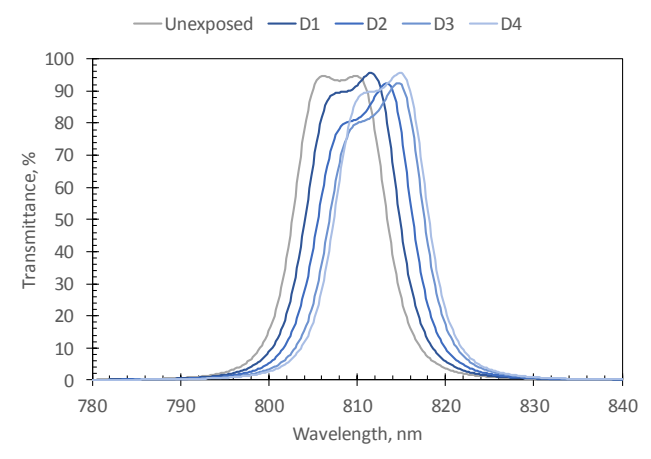

Figure 2. Theoretical evolution of the transmittance of a two-cavity quarter-wave layers bandpass filters for increasing of dosage of exposure at 470 nm (from a dosage D1 to D4).

Very similar shift and spectral transmission profiles can be observed theoretically when dosage is increased, confirming the origin of these distortions. To overcome this limitation, we therefore modified our approach. First, we opted for an exposure at a longer wavelength which is compatible with photo-inducing refractive index change in As_2S_3 layers. Indeed, we chose to expose at 532 nm, which is included within the absorption region of the As_2S_3 layer but in a lower absorbing region. That way, the absorption losses in these layers can be in, first approximation, neglected. In addition, we modified the Fabry-Perot structures in order to not only produce the expected bandpass function at 808 nm but also to secure an identical electric field distribution in both cavity layers at wavelength 532 nm, so that the central wavelengths of each cavity shifts similarly when exposed. Moreover, it is interesting to suppress the electric field oscillations across the cavities to achieve a uniform photo-induced refractive

index change throughout the layers' thicknesses. These standing wave oscillations comes from the fact that light propagates in both directions inside these layers. To suppress these oscillations, one must suppress backward propagation, which means that one side of the cavity layer must act as an antireflection coating at this wavelength. And in that case, the maximum electric field is achieved if the other side also acts as an antireflection coating.

Consequently, using internal design software based on needle optimization and our experience in designing such optical components, we calculated a new mirror structure that gives maximum transmittance at 808 nm to form the filter bandpass, and zero reflectance at 532 nm when considered between silica and As_2S_3. Silica being used for both the substrate and the coupling layers separating Fabry-Perot structures, such mirrors can be used all along the filter design. However, since air must be considered at last as the outer medium, a final silica/air antireflection structure must be added to the design, antireflection properties being required this time at both 532 and 808 nm wavelengths.

The new design of the structure can then be written:

Substrate / M'6 1.85C M'*6 L M'6 1.85C M'6* AR / Air

where M'6 and M'6*represent the new 6-layer mirrors that are used. M'6 mirrors have the following formula:

1.3H 0.662L 1.137H 1.086L 0.633H 1.323L

and M'6* mirrors have the same formula with layers in the reverse order. AR represents the final antireflection structure with following formula:

0.126H 0.346L 1.576H 0.766L

In these stack formulae, H, L and C respectively represent ZnS, YF_3 and As_2S_3 layers that are quarter wave at wavelength 808 nm. Note that the cavity layers are no more half-wave (but 1.85 times thicker) in order to account for the phase shift of these non-quarter-wave mirrors. We plotted in Figure 3 the normalized intensity distribution at 532 nm of this modified two-cavity Fabry-Perot filter:

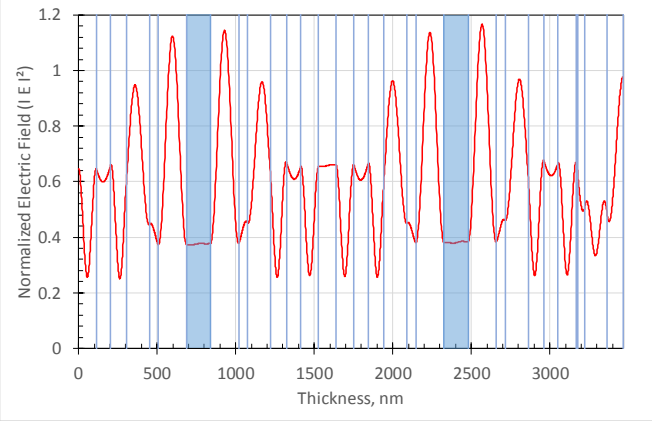

Figure 3. Normalized intensity distribution at 532 nm of the modified two-cavity Fabry-Perot filter. The cavities are highlighted.

As expected, the same electric field is achieved within the two cavities of the Fabry-Perot filter and modulation is close to zero due to the antireflection behavior of the structure at 532 nm. The electric field in the cavities is equal to 37% of the incident one. As the refractive index change is proportional to absorbed energy, achieving large photo-induced refractive index change only requires using larger exposure dosages.

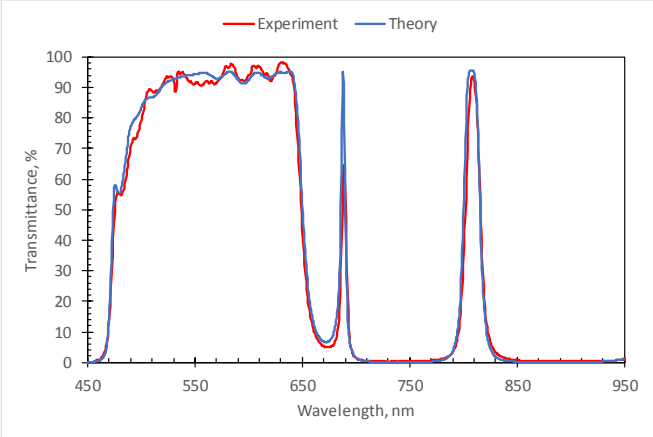

Figure 4. Experimental and theoretical transmittance of an optimized two-cavity bandpass filters.

This structure was then fabricated with the Bühler SYRUSpro machine. However, since the coating design is no more quarter-wave, turning point monitoring cannot be used. Consequently, in-situ trigger point optical monitoring has been used, at wavelengths within the bandpass region of the filter. While the optical monitoring of a bandpass filters with a full width at half maximum equal to larger than 10 nm can be achieved with actual monitoring techniques et methods, more complex optical monitoring strategies could be required for filters with narrower bandpass below 1 nm. Spectra before exposure are plotted in Figure 4. One can first see that we achieved a pretty good agreement between the theoretical and experimental transmittance over a broad spectral range. High transmission is obtained at 532 nm and 808 nm with a difference with theory not exceeding a few percent.

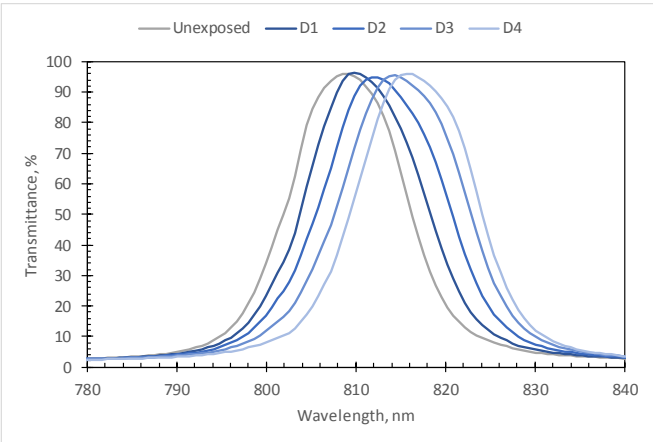

Figure 5. Experimental evolution of the of an optimized two-cavity bandpass filter as a function of dosage of exposure at 532 nm. The small insert shows an overlap of the measured spectra when numerically shifted to the same central wavelength.

Then, exposing the filter at 532 nm allows shifting the bandpass by about 10 nm without degrading the band pass profile (Figure 5). For this purpose, we used the same approach as before for determining D1 to D4. To illustrate the uniform shift of the bandpass, we also plotted in Figure 6, the spectral performances measured after increasing dosages at 532 nm when all wavelength scales are normalized for each filter by its central wavelength. Only very minor distortions of the transmittance, within the measurement accuracy, are observed.

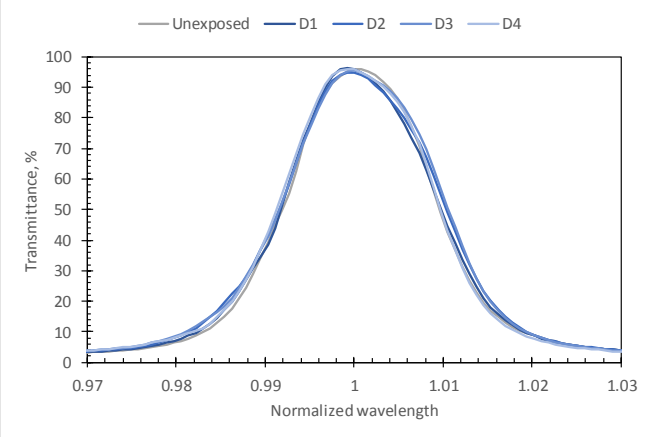

Figure 6. Spectral performances measured on an optimized two-cavity bandpass filter as a function of dosage of exposure at 532 nm when all wavelength scales are normalized for each filter by its central wavelength.

It is fundamental to note that adding a third identical cavity M'6/1.85C/M'6* to these two first ones maintains the antireflection properties at 532 nm. Therefore, the electric field is now identical in the three cavities, and so on for any number of cavities. In that way the proposed approach allows the design of filters with sharp band-pass profiles and high rejection characteristics that can be shifted without degradation of these optical properties.

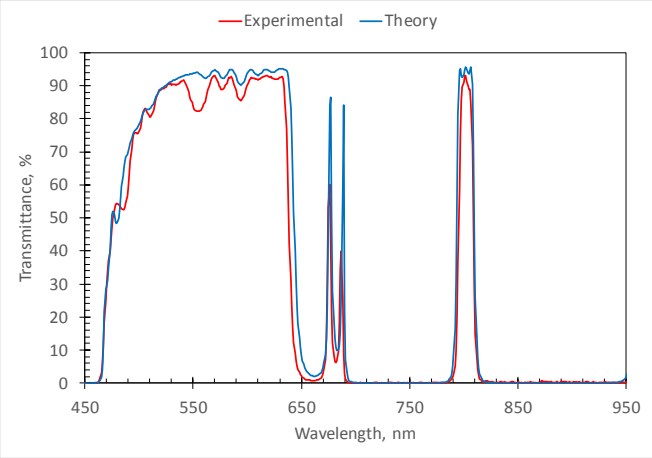

Figure 7. Experimental and theoretical transmittance of an optimized three-cavity bandpass filters.

To illustrate this concept, we manufactured a 3-cavity filter:

Substrate/M'6 1.85C M'6* L M'6 1.85C M'6* L M'6 1.85C M'6* AR / air

Measured spectral profiles before and after exposure are respectively plotted in Figures 7 and 8. One can first see that we still achieved a pretty good agreement between the theoretical and experimental transmittance over a broad spectral range. High transmission is once more obtained at 532 nm and 808 nm with a difference with theory not exceeding a few percent. Then, exposing the filter at 532 nm allows shifting the bandpass by about 10 nm without affecting the performances of the filter in the bandpass. Only very minor distortions of the transmittance within the measurement precision are observed.

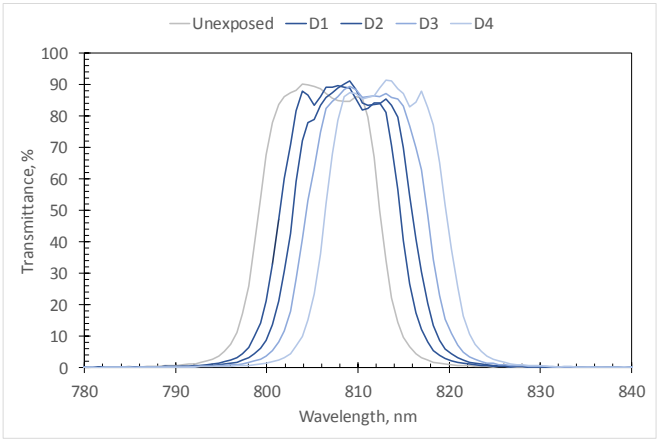

Figure 8. Experimental evolution of the transmittance of an optimized three-cavity bandpass filters as a function of dosage of exposure at 532 nm.

We have presented the design procedure and experimentally validated the concept of multi-cavity bandpass filters with bandpass that can be a-posteriori adjusted by photo-induced refractive index change. The calculated stack combines bandpass structure in transparency region and antireflection properties at laser-exposure wavelength. Using this method, we have shown high performance bandpass filters combining standard materials with chalcogenide, and tuning of the central wavelength without noticeable distortions in the spectral response of these filters. This method paves a way to the fabrication of highly uniform narrow-band filters.

Funding. Ministry for armed Forces (DGA), Aix-Marseille Université and A*Midex, an "Investissements d'Avenir" programme

Acknowledgement. Olivier Hector for his help with depositions.

Disclosures. The authors declare no conflicts of interest.

References

1. T. Begou, H. Krol, D. Stojcevski, F. Lemarchand, M. Lequime, C. Grezes-Besset and J. Lumeau, CEAS Space J 9(4), 441–449 (2017).
2. Michel Lequime, Remy Parmentier, Fabien Lemarchand, and Claude Amra, Appl. Opt. 41, 3277-3284 (2002)

3. M. Lequime and J. Lumeau, Advances in Optical Thin-Films (Jena, Germany), invited talk, paper 5963-08, September 2005
4. W.D. Shen, M. Cathelinaud, M. Lequime, V. Nazabal, and X. Liu, Opt. Commun., 281, 3726-3731 (2008)
5. A. Bourgade, and J. Lumeau, Optics Letters 44(2), 351-354 (2019).
6. P. Bousquet, A. Fornier, R. Kowalczyk, E. Pelletier, and P. Roche, Thin Solid Films13,285–290 (1972).
7. H. A. Macleod, Opt. Acta **19**, 1–28 (1972)
8. R. R. Willey, Appl. Opt.41,3193–3195 (2002).

References

1. T. Begou, H. Krol, D. Stojcevski, F. Lemarchand, M. Lequime, C. Grezes-Besset and J. Lumeau, "Complex optical interference filters with stress compensation for space applications", CEAS Space J 9(4), 441–449 (2017).
2. Michel Lequime, Remy Parmentier, Fabien Lemarchand, and Claude Amra, "Toward tunable thin-film filters for wavelength division multiplexing applications," Appl. Opt. 41, 3277-3284 (2002)
3. M. Lequime and J. Lumeau, "Laser trimming of thin-film filters", Advances in Optical Thin-Films (Jena, Germany), invited talk, paper 5963-08, September 2005
4. W.D. Shen, M. Cathelinaud, M. Lequime, V. Nazabal, and X. Liu, "Photosensitive post tuning of chalcogenide Te20As30Se50 narrow bandpass filters," Opt. Commun., 281, 3726-3731 (2008)
5. A. Bourgade, and J. Lumeau, "Large aperture, ultra-uniform, narrow bandpass filter based on As2S3 Fabry-Perot cavity", Optics Letters 44(2), 351-354 (2019).
6. P. Bousquet, A. Fornier, R. Kowalczyk, E. Pelletier, and P. Roche, “Optical filters: Monitoringprocess allowing the auto-correlation of thickness errors,” Thin Solid Films13,285–290 (1972).
7. H. A. Macleod, “Turning value monitoring of narrow-band all-dielectric thin-film optical filters”, Opt. Acta **19**, 1–28 (1972)
8. R. R. Willey, “Simulation of errors in the monitoring of narrow bandpass filters,” Appl. Opt.41,3193–3195 (2002).